

## Ferrocenyldiselenolate-Stabilized Copper–Selenium Clusters

Christian Nitschke,<sup>†</sup> Dieter Fenske,<sup>\*†‡</sup> and John F. Corrigan<sup>\*§</sup>

Institut für Anorganische Chemie der Universität Karlsruhe (TH), 76133 Karlsruhe, Germany, Forschungszentrum Karlsruhe in der Helmholtz-Gemeinschaft, 76344 Eggenstein-Leopoldshafen, Germany, and Department of Chemistry, The University of Western Ontario, London, N6A 5B7 Canada

Received June 20, 2006

The silylated ferrocenyl selenium reagent  $1,1'-\text{Fe}(\eta^5\text{-C}_5\text{H}_4\text{SeSiMe}_3)_2$  has been used for the high yield formation of the phosphine-ligated copper complexes  $\text{Cu}_2(\text{fcSe}_2)(\text{P}i\text{Pr}_3)_2$  (**1**) and  $\text{Cu}_4(\text{fcSe}_2)_2(\text{P}n\text{Pr}_3)_4$  (**2**) from solubilized  $\text{CuOAc}$ , as determined by single-crystal X-ray diffraction. The incorporation of a source of  $\text{Se}^{2-}$  into the reaction scheme with the reagent  $\text{Se}(\text{SiMe}_3)_2$  yields the mixed selenide/ferrocenyldiselenolate cluster  $[\text{Cu}_{20}\text{Se}_6(\text{Se}_2\text{fc})_4(\text{P}n\text{Pr}_3)_{10}]$  (**3**). Partial substitution of the  $\text{P}n\text{Pr}_3$  ligand shell in **3** with the phosphinothiol  $\text{Ph}_2\text{P}(\text{CH}_2)_3\text{SH}$  leads to an expansion of the framework and the high yield formation of the crystallographically characterized cluster  $\text{Cu}_{36}(\text{fcSe}_2)_6\text{Se}_{12}(\text{P}n\text{Pr}_3)_{10}(\text{Ph}_2\text{P}(\text{CH}_2)_3\text{SH})_2$  (**5**), which contains surface alkythiol groups on a copper–selenium core.

## Introduction

The utility and importance of silylated chalcogen reagents for the assembly of metal–chalcogenide and –chalcogenolate clusters continue to spur the development of this area of inorganic chemistry.<sup>1</sup> Investigations detailing the assembly of chalcogen-bridged nanometer-sized copper clusters (“nanoclusters”) have been described by using bis(trimethylsilyl)chalcogen reagents for the delivery of interstitial “ $\text{E}^{2-}$ ” ( $\text{E} = \text{S}, \text{Se}, \text{Te}$ ).<sup>2</sup> By varying the nature of the surface-stabilizing chalcogenolate ( $\text{RE}^-$ ) and phosphine ligands together with reaction conditions, one can isolate a large variety of core sizes ranging from the molecular to the nanoscale in single-crystalline form<sup>3</sup> and the optical and electronic properties of these  $\text{Cu}_2\text{E}$  clusters can be tuned by controlling the assembly of these monodisperse systems.<sup>2</sup> It was recently communicated that the surfaces of such clusters can be passivated and functionalized through the use of the

ferrocenyl reagent  $\text{Fe}(\text{C}_5\text{H}_4\text{SeSiMe}_3)_2$ ,<sup>4</sup> which serves as a soluble source of  $[\text{Fe}(\text{C}_5\text{H}_4\text{Se})_2]^{2-}$  ( $\text{fcSe}_2^{2-}$ ) during cluster-forming reactions. Although ferrocenyldiselenolate complexes of late transition metal complexes are well documented,<sup>5</sup> there are few reports describing the coordination of these ligands to group 11 metals.<sup>4,6</sup> Importantly,  $\text{fcSe}_2^{2-}$ -passivated copper–selenide semiconductor nanoclusters are relatively stable with respect to ligand dissociation/framework condensation reactions in solution, as the bidentate nature of the  $\text{fcSe}_2$  ligands assists in preventing random condensation

\* To whom correspondence should be addressed. E-mail: dieter.fenske@chemie.uni-karlsruhe.de (D.F.), corrigan@uwo.ca (J.F.C.). Phone: (+49)-721-608-2086 (D.F.), (+1)519-661-2111 ext. 86387 (J.F.C.).

<sup>†</sup> Institut für Anorganische Chemie der Universität Karlsruhe.

<sup>‡</sup> Forschungszentrum Karlsruhe in der Helmholtz-Gemeinschaft.

<sup>§</sup> The University of Western Ontario.

- (1) (a) DeGroot, M. W.; Corrigan, J. F. In *Comprehensive Coordination Chemistry 2*; Fujita, M., Powell, A. K., Creutz, C., Eds.; Elsevier: Oxford, U.K., 2004; Vol. 7, pp 57–113. (b) DeGroot, M. W.; Corrigan, J. F. In *The Chemistry of Nanomaterials: Synthesis, Properties, and Applications*; Rao, C. N. R. A., Müller, A., Cheetham, A. K., Eds.; Wiley-VCH: Weinheim, Germany, 2004; pp 418–451.
- (2) Dehnen, S.; Eichhöfer, A.; Fenske, D. *Eur. J. Inorg. Chem.* **2002**, 279–317.

- (3) (a) Fuhr, O.; Fernandez-Recio, L.; Fenske, D. *Eur. J. Inorg. Chem.* **2005**, 2306–2314. (b) Eichhöfer, A.; Beckmann, E.; Fenske, D.; Herein, D.; Krautscheid, H.; Schloegl, R. *Isr. J. Chem.* **2001**, *41*, 31–37. (c) Zhu, N.; Fenske, D. *J. Chem. Soc., Dalton Trans.* **1999**, 1067–1076. (d) Bettenhausen, M.; Eichhöfer, A.; Fenske, D.; Semmelmann, M. *Z. Anorg. Allg. Chem.* **1999**, 625, 593–601. (e) Eichhöfer, A.; Fenske, D. *J. Chem. Soc., Dalton Trans.* **1998**, 2969–2972. (f) Deveson, A.; Dehnen, S.; Fenske, D. *J. Chem. Soc., Dalton Trans.* **1997**, 4491–4498. (g) Corrigan, J. F.; Fenske, D. *Angew. Chem., Int. Ed. Engl.* **1997**, *36*, 1981–1983. (h) Dehnen, S.; Fenske, D. *Chem.—Eur. J.* **1996**, *2*, 1407–1416. (i) Corrigan, J. F.; Balter, S.; Fenske, D. *J. Chem. Soc., Dalton Trans.* **1996**, 729–738. (j) Krautscheid, H.; Fenske, D.; Baum, G.; Semmelmann, M. *Angew. Chem., Int. Ed. Engl.* **1993**, *32*, 1303–1305. (k) Fenske, D.; Krautscheid, H. *Angew. Chem., Int. Ed. Engl.* **1990**, *29*, 1452–1454.
- (4) (a) Wallbank, A. I.; Corrigan, J. F. *Chem. Commun.* **2001**, 377–378. (b) Wallbank, A. I.; Borecki, A.; Taylor, N. J.; Corrigan, J. F. *Organometallics* **2005**, *24*, 788–790.
- (5) (a) Brown, M. J.; Corrigan, J. F. *J. Organomet. Chem.* **2004**, 689, 2872–2879. (b) Herberhold, M.; Jin, G.-X.; Rheingold, A. L. *Z. Anorg. Allg. Chem.* **2002**, 628, 1985–1990. (c) Heberhold, M.; Jin, G.-X.; Rheingold, A. L.; Sheats, G. F. *Z. Naturforsch., B* **1992**, *47*, 1091–1098. (d) Matsuzaka, H.; Qu, J.-P.; Ogino, T.; Nishio, M.; Nishibayashi, Y.; Ishii, Y.; Uemura, S.; Hidai, M. *J. Chem. Soc., Dalton Trans.* **1996**, 4307–4312.
- (6) Wallbank, A. I.; Corrigan, J. F. *J. Cluster Sci.* **2004**, *15*, 225–232.

**Table 1.** Crystallographic Data for the Structure Determination of 1–6

param	1	2	3	4	5	6
chem formula	Cu <sub>2</sub> Se <sub>2</sub> FeP <sub>2</sub> C <sub>28</sub> H <sub>50</sub>	Cu <sub>4</sub> Se <sub>4</sub> Fe <sub>2</sub> P <sub>4</sub> C <sub>56</sub> H <sub>100</sub>	Cu <sub>20</sub> Se <sub>14</sub> Fe <sub>4</sub> P <sub>10</sub> C <sub>130</sub> H <sub>242</sub> ·C <sub>7</sub> H <sub>16</sub>	Cu <sub>2</sub> S <sub>4</sub> P <sub>4</sub> C <sub>60</sub> H <sub>66</sub>	Cu <sub>36</sub> Se <sub>24</sub> S <sub>1.7</sub> Fe <sub>6</sub> P <sub>12</sub> C <sub>178.2</sub> H <sub>293.2</sub>	Cu <sub>36</sub> Se <sub>24</sub> Fe <sub>6</sub> P <sub>12</sub> C <sub>204</sub> H <sub>276</sub>
fw	789.5	1578.9	4814.8	1166.3	7479.5	7617.5
space group	P2 <sub>1</sub> /n	P1̄	P1̄	P2 <sub>1</sub> /c	P2 <sub>1</sub> /n	P2 <sub>1</sub> /n
temp (°C)	–100	–173	–173	–123	–173	–173
a (Å)	10.5499(7)	13.211(3)	16.325(1)	12.9530(7)	19.763(3)	19.878(3)
b (Å)	12.443(1)	15.683(3)	18.020(1)	22.320(2)	21.774(2)	21.494(2)
c (Å)	25.042(2)	17.868(4)	18.004(1)	10.4615(5)	61.137(8)	61.897(10)
α (deg)	90	79.98(3)	79.962(5)	90	90	90
β (deg)	99.12(2)	79.34(3)	78.015(5)	112.431(4)	91.660(10)	92.280(10)
γ (deg)	90	67.29(3)	68.331(5)	90	90	90
V (Å <sup>3</sup> )	3245.7(4)	3334.6(11)	4787.5(5)	2795.7(3)	26297(6)	26425(6)
μ (Mo Kα <sub>1</sub> , mm <sup>–1</sup> )	4.097	3.988	5.242	1.063	6.605	6.562
Z	4	2	1	2	4	4
ρ (g cm <sup>–3</sup> )	1.616	1.572	1.670	1.386	1.859	1.915
data:params	7697:316	14663:626	15845:821	6661:320	21914:1423	39264:1427
R indices	R1 = 0.0555 [I > 2σ(I)] wR2 = 0.1461	R1 = 0.0466 wR2 = 0.1271	R1 = 0.0691 wR2 = 0.1879	R1 = 0.0442 wR2 = 0.1089	R1 = 0.0907 wR2 = 0.2538	R1 = 0.0911 wR2 = 0.2472

reactions from occurring when the clusters are dissolved in organic solvents, which can lead to amorphous products. Such systems could thus lend themselves to selective substitution reactions of the ancillary PR<sub>3</sub> ligands. The introduction of phosphine ligands containing thioether groups has been demonstrated;<sup>7</sup> however, to date, the introduction of a thiol group into the phosphine shell around such nanoclusters, which might allow covalent bonding onto a variety of metal surfaces via metal–thiolate bond formation,<sup>8</sup> has yet to be achieved. Herein, we describe the general assembly of high nuclearity ferrocenyldiselenolate clusters and nanoclusters of copper(I). We demonstrate that partial substitution of the ancillary phosphine ligand shell on Cu–Se frameworks is possible, leading to surface alkylthiol groups on a copper–selenide core.

### Experimental Section

**General Data.** All reactions were performed under an inert atmosphere of purified nitrogen using standard Schlenk techniques. Reagent grade solvents were dried by standard procedures and were freshly distilled prior to use. Deuterated solvents were dried over either potassium (C<sub>7</sub>D<sub>8</sub>, C<sub>6</sub>D<sub>6</sub>) or P<sub>2</sub>O<sub>5</sub> (CDCl<sub>3</sub>) under N<sub>2</sub>. CuOAc,<sup>9</sup> Ph<sub>2</sub>P(CH<sub>2</sub>)<sub>3</sub>SH,<sup>10</sup> PR<sub>3</sub>,<sup>11</sup> Se(SiMe<sub>3</sub>)<sub>2</sub>,<sup>12</sup> and fc(SeSiMe<sub>3</sub>)<sub>2</sub><sup>4a</sup> were prepared according to literature procedures.

The selection of single crystals suitable for X-ray diffraction was carried out by immersing the air-sensitive samples in perfluoropoly-

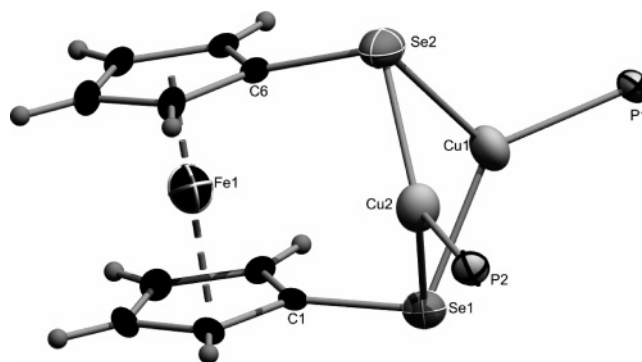


**Figure 1.** Molecular structure of Cu<sub>2</sub>(μ<sub>2</sub>-η<sup>2</sup>-fcSe<sub>2</sub>)(PiPr<sub>3</sub>)<sub>2</sub> (**1**) (isopropyl groups are omitted for clarity). The cyclopentadienyl rings of the ferrocenyl unit display an eclipsed arrangement.

**Table 2.** Selected Bond Distances (Å) and Angles (deg) for Cu<sub>2</sub>(μ<sub>2</sub>-η<sup>2</sup>-fcSe<sub>2</sub>)(PiPr<sub>3</sub>)<sub>2</sub> (**1**)

Se1–C1	1.895(4)
Se1–Cu1	2.3904(6)
Se1–Cu2	2.4816(8)
Se2–C6	1.898(4)
Se2–Cu2	2.4067(7)
Se2–Cu1	2.4567(7)
Cu1–P1	2.2167(11)
Cu2–P2	2.2081(11)
C1–Se1–Cu1	104.86(12)
C1–Se1–Cu2	100.26(12)
Cu1–Se1–Cu2	64.91(2)
C6–Se2–Cu2	99.95(12)
C6–Se2–Cu1	104.45(12)
Cu2–Se2–Cu1	65.06(2)
P1–Cu1–Se1	135.06(4)
P1–Cu1–Se2	117.81(4)
Se1–Cu1–Se2	103.69(3)
P2–Cu2–Se2	136.24(4)
P2–Cu2–Se1	119.82(4)
Se2–Cu2–Se1	102.47(2)
Se1–C1–Fe1	132.8(2)
Se2–C6–Fe1	133.0(2)

ether oil (Riedel de Hæn) and mounting the oil-coated crystal on a glass pin set in a goniometer head. The oil freezes upon cooling in a flow of nitrogen protecting the crystal from oxidation. The structural analyses were carried out at low temperatures (–100 to –173 °C) on a STOE IPDS II diffractometer (Mo Kα, λ = 0.710 73 Å) equipped with an imaging plate area detector (**3**, **4**, **6**) and on a STOE STADI 4 diffractometer (Mo Kα, λ = 0.710 73 Å) equipped with a four-circle CCD detector (**1**, **2**, **5**). Structure solution and refinement against F<sup>2</sup> were carried out using SHELXS and

- (7) Fuhr, O.; Meredith, A.; Fenske, D. *J. Chem. Soc., Dalton Trans.* **2002**, 4091–4094.  
 (8) Love, J. C.; Estroff, L. A.; Kriebel, J. K.; Nuzzo, R. G.; Whitesides, G. M. *Chem. Rev.* **2005**, *105*, 1103–1169.  
 (9) Edwards, D. A.; Richards, R. *J. Chem. Soc., Dalton Trans.* **1973**, 2463–2468.  
 (10) White, G. S.; Stephan, D. W. *Organometallics* **1987**, *6*, 2169–2175.  
 (11) (a) Cowley, A. H.; Mills, J. L. *J. Am. Chem. Soc.* **1969**, *91*, 2915–2919. (b) Cumper, C. W. N.; Foxton, A. A.; Read, J.; Vogl, A. I. *J. Chem. Soc.* **1964**, 430–434. (c) Grim, S. O.; McFarlane, W.; Davidoff, E. F. *J. Org. Chem.* **1967**, *32*, 781–784.  
 (12) DeGroot, M. W.; Taylor, N. J.; Corrigan, J. F. *J. Mater. Chem.* **2004**, *14*, 654–660.  
 (13) (a) Sheldrick, G. M. SHELXS-97: Program for Crystal Structure Solution. University of Göttingen, 1997. (b) Sheldrick, G. M. SHELXL-97: Program for Crystal Structure Refinement. University of Göttingen, 1997. (c) Sheldrick, G. M. SHELXP 5.05: Program for Molecular Graphics. University of Göttingen, 1994.  
 (14) Brandenburg, K.; Putz, H. DIAMOND Version 3.1: Crystal and Molecular Structure Visualization. Crystal Impact GbR: Bonn, Germany, 2005.

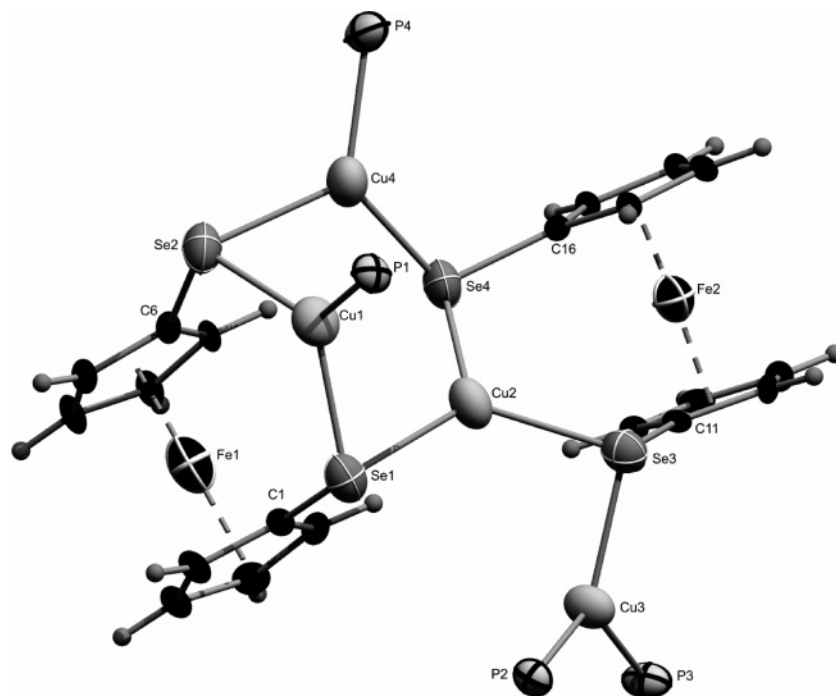


**Figure 2.** Molecular structure of  $\text{Cu}_4(\mu_3\text{-}\eta^2\text{-fcSe}_2)_2(\text{PnPr}_3)_4$  (**2**) (*n*-propyl groups are omitted for clarity). The cyclopentadienyl rings around Fe1 are in a near-eclipsed arrangement (deviation =  $3^\circ$ ), whereas the rings about Fe2 are staggered by  $51^\circ$ .

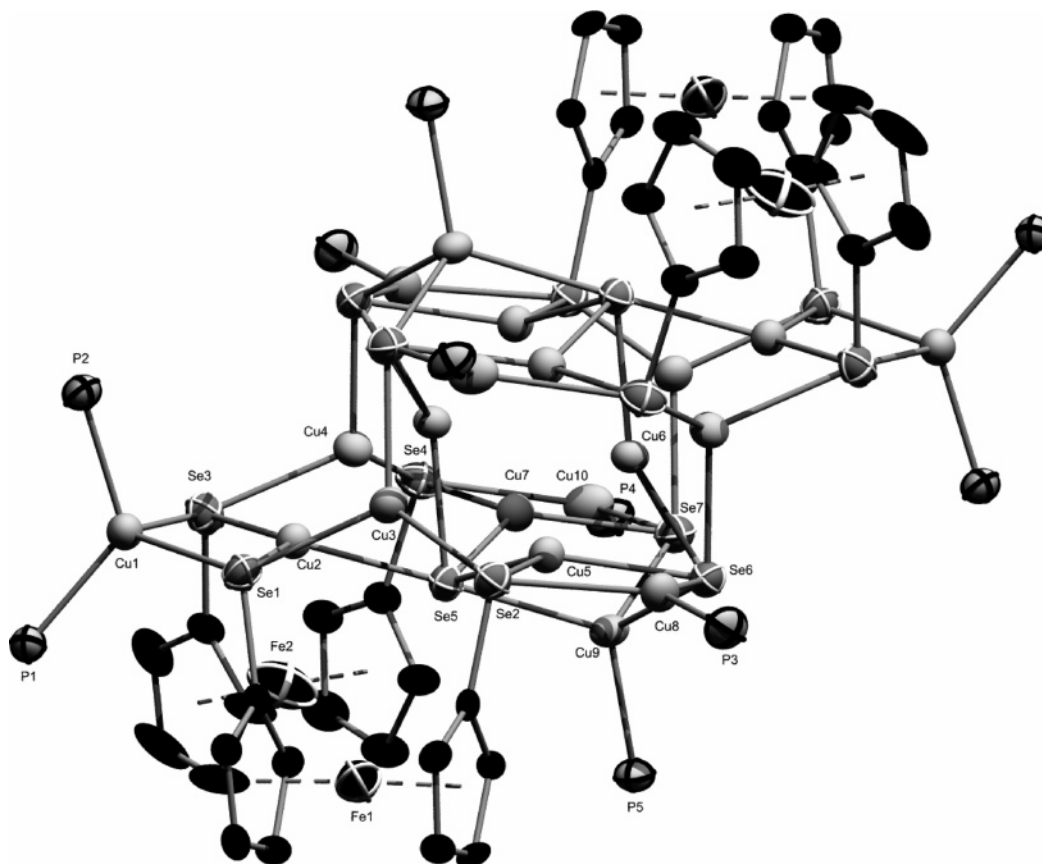


**Figure 3.** Molecular structure of  $\text{Cu}_{20}\text{Se}_6(\text{fcSe})_4(\text{PnPr}_3)_{10}$  (**3**) (propyl groups and H atoms are omitted for clarity).

SHELXL software.<sup>13</sup> Molecular diagrams were prepared using the DIAMOND 3.0 program.<sup>14</sup> The crystallographic data of **1–6** are summarized in Table 1. The weakly diffracting nature of crystals of **5** and **6** resulted in high  $R_1$  values. For **5**, site occupation (substitution) disorder was observed for one of the  $\text{Ph}_2\text{P}(\text{CH}_2)_3\text{SH}$

ligands (P6). A two-site  $\text{Ph}_2\text{P}(\text{CH}_2)_3\text{SH}:\text{PnPr}_3$  model (70:30) gave a satisfactory refinement.

$^1\text{H}$  and  $^{31}\text{P}\{^1\text{H}\}$  NMR spectra were recorded on either a Bruker AMX 300 or an AV 400 spectrometer. Spectra are referenced internally to residual protio-solvent ( $^1\text{H}$ ) or externally ( $^{31}\text{P}$ ) and are

**Table 3.** Selected Bond Distances (Å) and Angles (deg) for  $\text{Cu}_4(\text{fcSe}_2)_2(\text{PnPr}_3)_4$  (**2**)

Se1–Cu1	2.3462(11)
Se1–Cu2	2.3716(13)
Se2–Cu4	2.3477(13)
Se2–Cu2	2.3689(12)
Se3–Cu3	2.3521(11)
Se3–Cu2	2.3892(11)
Se4–Cu3	2.3338(12)
Se4–Cu4	2.3987(11)
Cu1–P2	2.2341(17)
Cu1–P1	2.2381(18)
Cu3–P4	2.2088(17)
Cu4–P3	2.217(2)
C1–Se1–Cu1	102.77(17)
C1–Se1–Cu2	103.69(18)
Cu1–Se1–Cu2	94.20(4)
C6–Se2–Cu4	110.03(16)
C6–Se2–Cu2	107.76(17)
Cu4–Se2–Cu2	104.75(5)
C16–Se3–Cu3	109.85(18)
C16–Se3–Cu2	100.01(17)
Cu3–Se3–Cu2	75.78(4)
C11–Se4–Cu3	108.14(17)
C11–Se4–Cu3	107.63(18)
Cu3–Se4–Cu4	71.24(4)
P2–Cu1–P1	123.41(7)
P2–Cu1–Se1	117.03(5)
P1–Cu1–Se1	117.61(6)
Se2–Cu2–Se1	116.27(4)
Se2–Cu2–Se3	120.11(5)
Se1–Cu2–Se3	123.29(4)
P4–Cu3–Se4	125.83(6)
P4–Cu3–Se3	110.36(6)
Se4–Cu3–Se3	120.83(4)
P3–Cu4–Se2	125.90(6)
P3–Cu4–Se4	120.20(7)
Se2–Cu4–Se4	111.88(5)
Se1–C1–Fe1	126.5(3)
Se2–C6–Fe1	123.6(3)
Se4–C11–Fe2	135.5(3)
Se3–C16–Fe2	134.0(3)

reported relative to tetramethylsilane ( $^1\text{H}$ ) or 85% phosphoric acid ( $^{31}\text{P}$ ). Chemical shifts are quoted in  $\delta$  (ppm) and coupling constants in Hertz.

UV–vis spectra were recorded with a Perkin-Elmer UV/VIS/NIR Spectrometer Lambda 900 at room temperature as solutions in dichloromethane. Elemental analysis was performed with a Vario EL-Analysensautomaten “elementar Vario EL” by ELEMENTAR-Analysensysteme.

**Synthesis of  $\text{Cu}_2(\text{fcSe}_2)(\text{PiPr}_3)_2$  (**1**).**  $\text{PiPr}_3$  (1.33 mL, 7.05 mmol) was added to a suspension of  $\text{CuOAc}$  (0.42 g, 3.4 mmol) in 20 mL of THF to yield a clear, colorless solution. The reaction was cooled to  $-65^\circ\text{C}$ , and a solution of  $\text{fc}(\text{SeSiMe}_3)_2$  (0.82 g, 1.7 mmol, dissolved in 7 mL of THF) was added. Slow warming to room temperature over 4 days afforded a light brown solution. Layering with *n*-pentane afforded yellow-orange blocks of **1** in 65% yield based on Cu. Anal. Calcd for **1**: C, 42.60; H, 6.38. Found: C, 42.31; H, 6.33.  $^1\text{H}$  NMR ( $\text{C}_6\text{D}_6$ , 298 K,  $\delta$ ): 4.21 (t,  $J_{\text{HH}} = 2$  Hz, 4H), 4.11 (t,  $J_{\text{HH}} = 2$  Hz, 4H), 1.80 (m, 6H, P–CH–), 1.12 (m, 36H,  $-\text{CH}_3$ ).  $^{31}\text{P}\{^1\text{H}\}$ -NMR ( $\text{C}_6\text{D}_6$ ,  $\delta$ ):  $-22.2$  (br s,  $W_{1/2} = 53$  Hz). UV–vis: 453 nm (sh,  $\epsilon = 170$  L mol $^{-1}$  cm $^{-1}$ ).

**Synthesis of  $\text{Cu}_4(\text{fcSe}_2)_2(\text{PnPr}_3)_4$  (**2**).**  $\text{CuOAc}$  (0.20 g, 1.6 mmol) was dissolved with  $\text{PnPr}_3$  (0.65 mL, 3.56 mmol) in 15 mL of THF. The solution was cooled to  $-65^\circ\text{C}$ , and a solution of  $\text{fc}(\text{SeSiMe}_3)_2$  (0.42 g, 0.85 mmol, dissolved in 3 mL of THF) was added. Slow warming to room temperature over 4 days afforded a brown solution. Layering with *n*-pentane led to X-ray-quality orange-red crystals of **2** in 70% yield based on Cu. Anal. Calcd for **2**: C,

**Table 4.** Selected Bond Distances (Å) and Angles (deg) for  $\text{Cu}_{20}\text{Se}_6(\text{fcSe}_2)_4(\text{PnPr}_3)_{10}$  (**3**)

Cu1–Se3	2.5895(16)	P3–Cu8–Se2	106.03(9)
Cu1–Se1	2.6791(16)	Se6–Cu8–Se2	119.10(6)
Cu2–Se1	2.3987(14)	P5–Cu9–Se6	108.69(10)
Cu2–Se5	2.4206(14)	P5–Cu9–Se7	112.39(10)
Cu2–Se3	2.4242(15)	Se6–Cu9–Se7	97.24(5)
Cu3–Se7 <sup>a</sup>	2.3940(14)	P5–Cu9–Se5	117.66(9)
Cu3–Se2	2.4010(14)	Se6–Cu9–Se5	109.22(5)
Cu3–Se1	2.4301(15)	Se7–Cu9–Se5	109.66(5)
Cu4–Se4	2.3987(15)	P4–Cu10–Se7	135.05(10)
Cu4–Se6 <sup>a</sup>	2.3991(14)	P4–Cu10–Se4	105.92(10)
Cu4–Se3	2.4391(15)	Se7–Cu10–Se4	117.81(6)
Cu5–Se5	2.4037(16)	Cu2–Se1–Cu3	70.16(5)
Cu5–Se6	2.4834(14)	Cu2–Se1–Cu1	60.42(4)
Cu5–Se2	2.5228(14)	Cu3–Se1–Cu1	122.12(5)
Cu6–Se5	2.4768(13)	Cu3–Se2–Cu5	65.52(4)
Cu6–Se6 <sup>a</sup>	2.6034(14)	Cu3–Se2–Cu8	123.26(5)
Cu6–Se7 <sup>a</sup>	2.6222(15)	Cu5–Se2–Cu8	60.20(4)
Cu7–Se5	2.3943(14)	Cu2–Se3–Cu4	69.03(5)
Cu7–Se7	2.4561(14)	Cu2–Se3–Cu1	61.47(4)
Cu7–Se4	2.5243(16)	Cu4–Se3–Cu1	123.44(6)
Cu8–Se6	2.3556(16)	Cu4–Se4–Cu7	64.58(5)
Cu8–Se2	2.5826(14)	Cu4–Se4–Cu10	122.91(6)
Cu9–Se6	2.5146(17)	Cu7–Se4–Cu10	60.31(4)
Cu9–Se7	2.5176(15)	Cu7–Se5–Cu5	104.41(5)
Cu9–Se5	2.6095(14)	Cu7–Se5–Cu2	116.24(5)
Cu9–Cu6 <sup>a</sup>	2.6711(15)	Cu5–Se5–Cu2	114.40(5)
Cu10–Se7	2.3691(17)	Cu7–Se5–Cu6	77.65(4)
Cu10–Se4	2.5989(16)	Cu5–Se5–Cu6	73.81(5)
Se6–Cu4 <sup>a</sup>	2.3991(14)	Cu2–Se5–Cu6	67.95(4)
Se6–Cu6 <sup>a</sup>	2.6034(14)	Cu7–Se5–Cu9	64.50(4)
Se7–Cu3 <sup>a</sup>	2.3940(14)	Cu5–Se5–Cu9	66.01(4)
Se7–Cu6 <sup>a</sup>	2.6222(15)	Cu2–Se5–Cu9	178.82(5)
P1–Cu1–P2	122.82(11)	Cu6–Se5–Cu9	113.21(5)
P1–Cu1–Se3	105.13(9)	Cu8–Se6–Cu4 <sup>a</sup>	74.51(5)
P2–Cu1–Se3	105.75(8)	Cu8–Se6–Cu5	63.84(4)
P1–Cu1–Se1	110.28(8)	Cu4 <sup>a</sup> –Se6–Cu5	79.05(5)
P2–Cu1–Se1	102.24(9)	Cu8–Se6–Cu9	120.43(5)
Se3–Cu1–Se1	110.34(5)	Cu4 <sup>a</sup> –Se6–Cu9	124.69(5)
Se1–Cu2–Se5	115.26(5)	Cu5–Se6–Cu9	66.38(5)
Se1–Cu2–Se3	127.46(6)	Cu8–Se6–Cu6 <sup>a</sup>	116.48(5)
Se5–Cu2–Se3	114.83(6)	Cu4 <sup>a</sup> –Se6–Cu6 <sup>a</sup>	63.31(4)
Se7 <sup>a</sup> –Cu3–Se2	118.14(6)	Cu5–Se6–Cu6 <sup>a</sup>	63.25(4)
Se7 <sup>a</sup> –Cu3–Se1	113.82(5)	Cu9–Se6–Cu6 <sup>a</sup>	62.89(4)
Se2–Cu3–Se1	114.96(5)	Cu10–Se7–Cu3 <sup>a</sup>	79.79(5)
Se4–Cu4–Se6 <sup>a</sup>	120.75(6)	Cu10–Se7–Cu7	64.47(5)
Se4–Cu4–Se3	112.70(6)	Cu3 <sup>a</sup> –Se7–Cu7	81.73(5)
Se6 <sup>a</sup> –Cu4–Se3	109.81(5)	Cu10–Se7–Cu9	118.35(6)
Se5–Cu5–Se6	117.47(6)	Cu3 <sup>a</sup> –Se7–Cu9	124.33(5)
Se5–Cu5–Se2	118.75(5)	Cu7–Se7–Cu9	65.09(4)
Se6–Cu5–Se2	116.57(5)	Cu10–Se7–Cu6 <sup>a</sup>	118.58(5)
Se5–Cu7–Se7	119.56(6)	Cu3 <sup>a</sup> –Se7–Cu6 <sup>a</sup>	62.83(4)
Se5–Cu7–Se4	117.48(5)	Cu7–Se7–Cu6 <sup>a</sup>	63.43(4)
Se7–Cu7–Se4	117.41(5)	Cu9–Se7–Cu6 <sup>a</sup>	62.59(4)
P3–Cu8–Se6	134.58(10)		

<sup>a</sup> Symmetry transformations used to generate equivalent atoms:  $-x, -y, -z$ .

42.60; H, 6.38. Found: C, 42.83; H, 6.38.  $^1\text{H}$  NMR ( $\text{C}_7\text{D}_8$ , 193 K,  $\delta$ ): 5.18 (1H), 4.94 (1H), 4.73 (1H), 4.58 (1H), 4.53 (1H), 4.50 (1H), 4.42 (1H), 4.34 (1H), 4.29 (1H), 4.27 (1H), 4.09 (1H), 4.03 (1H), 3.94 (1H), 3.87 (1H), 3.82 (1H), 3.68 (1H), 1.50–1.07 (br, 84H).  $^{31}\text{P}\{^1\text{H}\}$ -NMR ( $\text{C}_7\text{D}_8$ , 223 K,  $\delta$ ):  $-20.5$  (s),  $-21.0$  (s),  $-22.4$  (s) (intensity 1:1:2). UV–vis: 460 nm (sh,  $\epsilon = 673$  L mol $^{-1}$  cm $^{-1}$ ).

**Synthesis of  $\text{Cu}_{20}\text{Se}_6(\text{fcSe}_2)_4(\text{PnPr}_3)_{10}$  (**3**).**  $\text{CuOAc}$  (0.76 g, 6.2 mmol) was dissolved with  $\text{PnPr}_3$  (2.44 mL, 12.4 mmol) in 25 mL of THF. The solution was cooled to  $-65^\circ\text{C}$ , and  $\text{Se}(\text{SiMe}_3)_2$  (0.52 mL, 2.1 mmol) and a solution of  $\text{fc}(\text{SeSiMe}_3)_2$  (0.50 g, 1.0 mmol, dissolved in 4 mL of THF) were added. Slow warming to room temperature over 4 days afforded a brown solution, and removal of the solvent under reduced pressure led to a brown powder. The

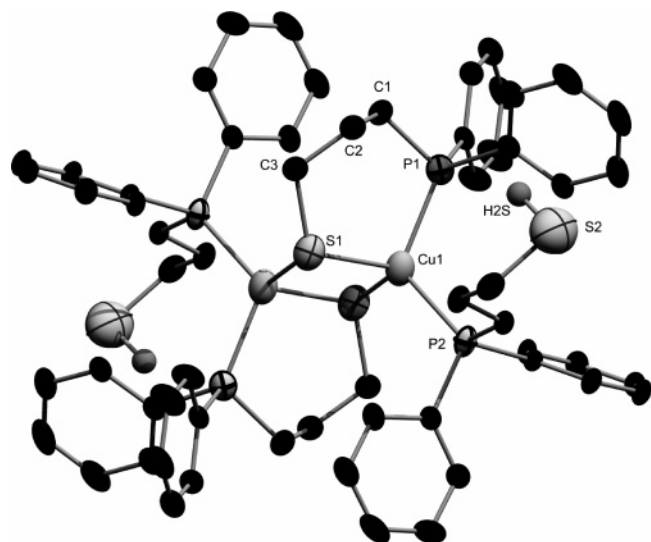


**Figure 4.** Molecular structure of  $\text{Cu}_2(\mu_2\text{-}\eta^2\text{-Ph}_2\text{P}(\text{CH}_2)_3\text{S})_2(\text{Ph}_2\text{P}(\text{CH}_2)_3\text{SH})_2$  (**4**).

powder was redissolved in *n*-heptane, and the resulting solution was filtered. Cluster **3** crystallized out of saturated solutions at room temperature as X-ray-quality brown blocks in 75% yield based on Cu. Anal. Calcd for **3**: C, 33.12; H, 5.17. Found: C, 32.85; H, 5.12.  $^1\text{H}$  NMR ( $\text{CDCl}_3$ , ferrocenyl region,  $\delta$ ): 4.83 (s, 4H), 4.67 (s, 4H), 4.07–3.90 (m, 24 H).  $^{31}\text{P}\{^1\text{H}\}$ -NMR ( $\text{C}_7\text{D}_8$ ,  $\delta$ ): –23.7 ppm (br, s).

**Synthesis of  $\text{Cu}_2(\text{Ph}_2\text{P}(\text{CH}_2)_3\text{S})_2(\text{Ph}_2\text{P}(\text{CH}_2)_3\text{SH})_2$  (**4**).**  $\text{Ph}_2\text{P}(\text{CH}_2)_3\text{SH}$  (1.31 mL, 5.64 mmol) was added to a suspension of  $\text{CuOAc}$  (0.23 g, 1.9 mmol) in 10 mL of diethyl ether. Storing

**Table 5.** Selected Bond Distances (Å) and Angles (deg) for  $\text{Cu}_2(\text{Ph}_2\text{P}(\text{CH}_2)_3\text{S})_2(\text{Ph}_2\text{P}(\text{CH}_2)_3\text{SH})_2$  (**4**)

Cu1–P2	2.2605(7)
Cu1–P1	2.2636(9)
Cu1–S1	2.3756(8)
Cu1–S1 <sup>a</sup>	2.3776(7)
S1–C3	1.831(3)
S1–Cu1 <sup>a</sup>	2.3776(7)
S2–C18	1.784(4)
P2–Cu1–P1	115.57(3)
P2–Cu1–S1	111.56(3)
P1–Cu1–S1	102.25(3)
P2–Cu1–S1 <sup>a</sup>	112.51(3)
P1–Cu1–S1 <sup>a</sup>	112.09(3)
S1–Cu1–S1 <sup>a</sup>	101.46(3)
C3–S1–Cu1	111.99(12)
C3–S1–Cu1 <sup>a</sup>	112.82(11)
Cu1–S1–Cu1 <sup>a</sup>	78.54(2)

<sup>a</sup> Symmetry transformations used to generate equivalent atoms:  $-x, -y + 1, -z + 1$ .

the solution at 0 °C yielded crystalline **6** as yellow crystals in 90% yield based on Cu. Anal. Calcd for **4**: C, 61.78; H, 5.70. Found: C, 61.96; H, 5.78.  $^1\text{H}$  NMR ( $\text{C}_6\text{D}_6$ ,  $\delta$ ): 7.57 (br s, 16H), 7.03 (br s, 24 H), 2.04 (br s, 12H,  $\text{CH}_2$ ), 1.70 (br s, 12H,  $\text{CH}_2$ ), 1.07 (br s, 2H, SH).  $^{31}\text{P}\{^1\text{H}\}$ -NMR ( $\text{C}_6\text{D}_6$ ,  $\delta$ ): –15.5 (s). UV–vis: 279 nm ( $\epsilon = 2290 \text{ L mol}^{-1} \text{ cm}^{-1}$ ).

**Synthesis of  $\text{Cu}_{36}(\text{fcSe}_2)_6\text{Se}_{12}(\text{PnPr}_3)_{10}(\text{Ph}_2\text{P}(\text{CH}_2)_3\text{SH})_2$  (**5**).** **3** (0.12 g, 0.025 mmol) was dissolved in a mixture of 15 mL diethyl ether:THF (2:1). To the resulting dark brown solution was added at room temperature a large excess of  $\text{Ph}_2\text{P}(\text{CH}_2)_3\text{SH}$  (0.12 mL, 0.51 mmol). The reaction mixture was allowed to stir overnight. After slow diffusion of 10 mL of pentane into the mixture, the reaction was stored at –35 °C. After 1 week, cluster **5** was retrieved

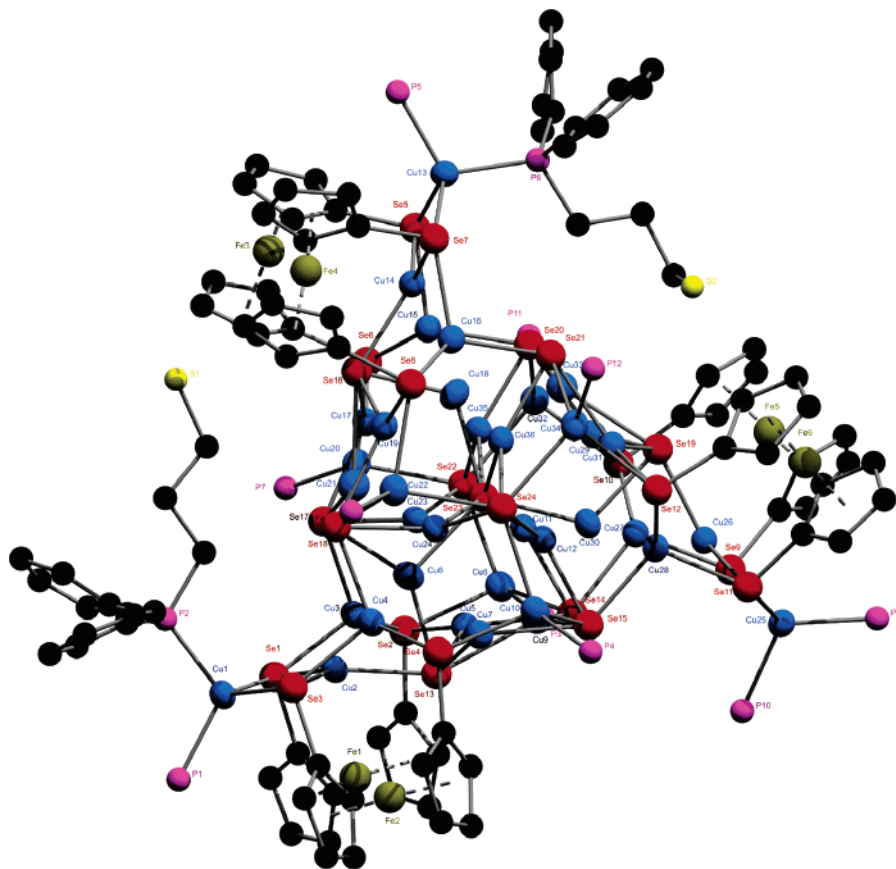


**Figure 5.** Molecular structure of  $\text{Cu}_{36}\text{Se}_{12}(\text{fcSe}_2)_6(\text{PnPr}_3)_{10}(\text{Ph}_2\text{P}(\text{CH}_2)_3\text{SH})_2$  (**5**) (propyl groups and H atoms are omitted for clarity).

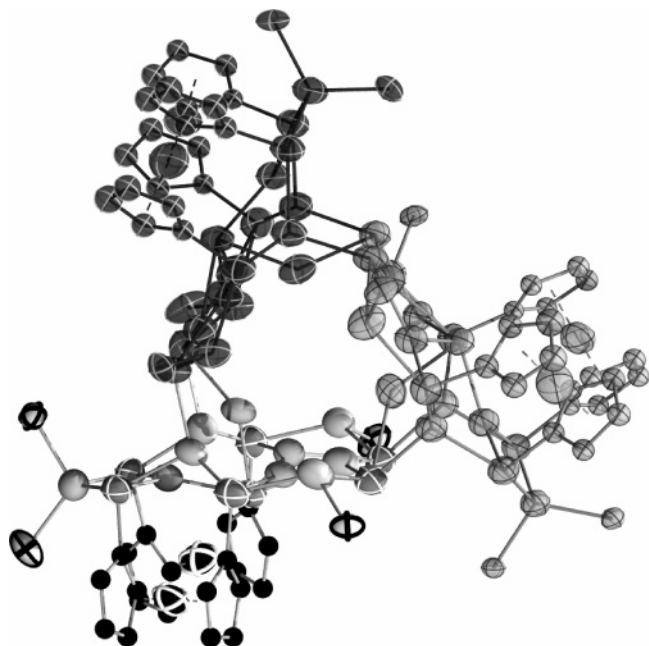


**Figure 6.** Three subunits of the surface of  $\text{Cu}_{36}\text{Se}_{12}(\text{fcSe}_2)_6(\text{PnPr}_3)_{10}(\text{Ph}_2\text{P}(\text{CH}_2)_3\text{SH})_2$  (**5**) emphasizing the relationship to the arrangement of atoms observed on the surface of cluster **3** (phosphorus substituents and all H atoms are omitted for clarity).

as dark brown X-ray-quality needles in 78% yield. Anal. Calcd for **5**: C, 29.00; H, 4.00. Found: C, 29.25; H, 3.92

**Synthesis of  $\text{Cu}_{36}\text{Se}_{12}(\text{fcSe}_2)_6(\text{PnPr}_2\text{Ph})_{12}$  (**6**).**  $\text{CuOAc}$  (0.40 g, 3.3 mmol) was dissolved with  $\text{PnPr}_2\text{Ph}$  (1.40 mL, 6.50 mmol) in 25 mL of THF. The solution was cooled to  $-65^\circ\text{C}$ , and  $\text{Se}(\text{SiMe}_3)_2$  (0.22 mL, 0.98 mmol) and a solution of  $\text{fc}(\text{SeSiMe}_3)_2$  (0.31 g, 0.64 mmol, dissolved in 4 mL THF) were added. The solution was warmed to room temperature over a period of 3–4 days to give a brown solution. Slow diffusion of *n*-pentane into the solution afforded **6** as X-ray-quality dark brown needles in 32% yield based on Cu. Anal. Calcd for **6**: C, 32.16; H, 3.65. Found: C, 32.29; H, 3.58.

## Results and Discussion

Copper(I) acetate is dissolved in common organic solvents with the use of tertiary phosphine ligands and reacts readily with trimethylsilyl–selenium reagents via the formation of metal–selenium bonds and the formation of trimethylsilyl acetate.<sup>2</sup> The silane byproduct of these reactions does not interfere with the crystallization process of the formed cluster and, most importantly, nanocluster complexes. Thus, when  $\text{CuOAc}$  was dissolved in THF with  $\text{PiPr}_3$  and reacted with  $\text{fc}(\text{SeSiMe}_3)_2$ , the dimeric complex  $\text{Cu}_2(\mu_2\text{-}\eta^2\text{-fcSe}_2)(\text{PiPr}_3)_2$  (**1**) was isolated in good yield after the addition of pentane. The structure of **1** is illustrated in Figure 1, and selected bond lengths are presented in Table 2. The two copper atoms show a distorted trigonal planar arrangement (sum of the angles  $357^\circ$  (Cu1) and  $359^\circ$  (Cu2), each bonded to two selenium centers of the ferrocenyl unit and one  $\text{PiPr}_3$  ligand. The selenolate centers each asymmetrically bridge the two copper sites, and the two cyclopentadienyl ligands adopt an eclipsed arrangement. Although the two  $\text{C}_5$  rings about iron are nearly parallel (deviation =  $2.0^\circ$ ), the two Se centers lie slightly above the cyclopentadienyl rings to which they are

bonded (0.2 Å). The two selenolate bridges are somewhat asymmetrically ligated to the two metals (Table 2) with the  $\text{Cu}\cdots\text{Cu}$  distance (2.6155(8) Å) in accord with the +1 oxidation states. The solution  $^1\text{H}$  NMR spectra for **1** are consistent with the observed solid-state structure, with two sharp signals observed in the ferrocenyl region at room temperature ( $\delta = 4.21, 4.11$  ppm), similar to those reported for ferrocenyldichalcogenolates bridging two metal centers.<sup>15</sup>

The reaction of  $\text{CuOAc}$  solubilized with the smaller trialkylphosphine  $\text{PnPr}_3$  and  $\text{fc}(\text{SeSiMe}_3)_2$  led to the selective formation of the cluster  $\text{Cu}_4(\text{fcSe}_2)_2(\text{PnPr}_3)_4$  (**2**) (Figure 2). As observed in **1**, each copper center displays a distorted trigonal planar coordination geometry, with angles varying from  $110.5^\circ$  ( $\text{P4-Cu3-Se3}$ ) to  $125^\circ$  ( $\text{P4-Cu3-Se4}$ ) (Table 3). In **2**, however, this is achieved with an asymmetric distribution of the phosphine ligands and bridging selenolate bonds. Whereas Cu1 and Cu4 are each coordinated to two Se and one phosphine ligand, Cu2, which is located in the center of the cluster, is bonded to three selenium atoms (Se1, Se2, Se3) and the trigonal coordination about Cu3 is achieved with one selenium (Se1) and two phosphine ligands. The structure of **2** can be described as a dimerization of **1** (with a different distribution of the  $\text{PR}_3$  ligands), likely due to the reduced steric requirements of  $\text{PnPr}_3$  versus  $\text{PiPr}_3$ .<sup>16</sup> At 223 K,  $^1\text{H}$  NMR spectra of **2** display 16 well-resolved signals for the inequivalent  $\text{C}_5\text{H}_4$  protons. **1** and **2** represent rare examples of copper–ferrocenyldiselenolate complexes.<sup>4</sup>

Using a combination of  $\text{fc}(\text{SeSiMe}_3)_2$  together with  $\text{Se}(\text{SiMe}_3)_2$  allows for the formation of larger frameworks, due to the formation and availability of  $\text{Se}^{2-}$  for the generation of a copper–selenide core, which can then be passivated via the introduction of surface selenolate ligands.<sup>1,2</sup> Thus, the reaction of  $\text{CuOAc}\cdot 2\text{PnPr}_3$  with a mixture of  $\text{fc}(\text{SeSiMe}_3)_2$  and  $\text{Se}(\text{SiMe}_3)_2$  (6:1:2) leads to the high yield formation of the mixed selenide/ferrocenyldiselenolate nanocluster  $\text{Cu}_{20}\text{Se}_6(\text{fcSe}_2)_4(\text{PnPr}_3)_{10}$  (**3**). The Cu–Se framework of **3** (Table 4) is similar to that which was previously communicated for the complexes  $\text{Cu}_{20}\text{Se}_6(\text{fcSe}_2)_4(\text{PnBu}_3)_{10}$  and  $\text{Cu}_{20}\text{Se}_6(\text{fcSe}_2)_4(\text{PEt}_2\text{Ph})_{10}$ , with only minor deviations due to the different tertiary phosphine ligands employed.<sup>4b</sup> The selenium framework consists of six  $\mu_5$ -selenide ligands (Se5, Se6, Se7, and their symmetry equivalents) arranged to form an (nonbonded) octahedron at the center of the clusters, which, in addition to the central ring of the four  $\text{fcSe}_2^{2-}$  groups, are bonded to the copper(I) centers (Figure 3). The ferrocenyldiselenolate ligands are each bonded to three copper sites, and the copper centers display both trigonal and tetrahedral coordination geometries.

We observe that solutions of **3** are kinetically stable under ambient conditions, as shown by NMR spectroscopy and

(15) (a) Takemoto, S.; Kuwata, S.; Nishibayashi, Y.; Hidai, M. *Organometallics* **2000**, *19*, 3249–3252. (b) Takemoto, S.; Kuwata, S.; Nishibayashi, Y.; Hidai, M. *Inorg. Chem.* **1998**, *37*, 6428–6434. (c) Herberhold, M.; Jin, G.-X.; Rheingold, A. L. *Angew. Chem., Int. Ed. Engl.* **1995**, *34*, 656–657. (d) Heberhold, M.; Jin, G.-X.; Rheingold, A. L.; Sheats, G. F. *Z. Naturforsch., B* **1992**, *47*, 1091–1098. (e) Cullen, W. R.; Talaba, A.; Rettig, S. J. *Organometallics* **1992**, *11*, 3152–3156. (f) Seyferth, D.; Hames, B. W. *Inorg. Chim. Acta* **1983**, *77*, L1–L2.

(16) Tolman, C. A. *Chem. Rev.* **1977**, *77*, 312–348.

**Table 6.** Selected Bond Distances (Å) for  $\text{Cu}_{36}(\text{fcSe}_2)_6\text{Se}_{12}(\text{PPr}_3)_{10}(\text{Ph}_2\text{P}(\text{CH}_2)_3\text{SH})_2$  (**5**)

Cu1–Se3	2.544(4)	Cu19–Se18	2.624(5)
Cu1–Se1	2.573(4)	Cu20–Se6	2.443(5)
Cu2–Se13	2.425(4)	Cu20–Se22	2.586(5)
Cu2–Se3	2.424(4)	Cu20–Se17	2.897(5)
Cu2–Se1	2.438(4)	Cu21–Se18	2.335(5)
Cu3–Se2	2.390(4)	Cu21–Se17	2.360(4)
Cu3–Se1	2.402(4)	Cu21–Se16	2.687(5)
Cu3–Se17	2.415(4)	Cu22–Se8	2.522(5)
Cu4–Se4	2.404(4)	Cu22–Se18	2.556(4)
Cu4–Se3	2.410(4)	Cu22–Se24	2.602(4)
Cu4–Se18	2.415(5)	Cu23–Se17	2.316(4)
Cu5–Se13	2.432(4)	Cu23–Se22	2.395(4)
Cu5–Se2	2.458(4)	Cu23–Se23	2.882(4)
Cu5–Se14	2.566(4)	Cu24–Se18	2.359(4)
Cu6–Se13	2.404(5)	Cu24–Se24	2.507(4)
Cu6–Se23	2.552(4)	Cu24–Se23	2.709(4)
Cu6–Se17	2.815(5)	Cu25–Se11	2.566(4)
Cu7–Se13	2.424(4)	Cu25–Se9	2.566(4)
Cu7–Se4	2.452(4)	Cu26–Se19	2.423(4)
Cu7–Se15	2.585(4)	Cu26–Se11	2.429(4)
Cu8–Se2	2.503(5)	Cu26–Se9	2.437(4)
Cu8–Se22	2.565(5)	Cu27–Se10	2.398(4)
Cu8–Se14	2.704(5)	Cu27–Se9	2.402(4)
Cu9–Se15	2.343(5)	Cu27–Se14	2.414(4)
Cu9–Se14	2.355(4)	Cu28–Se12	2.392(4)
Cu9–Se13	2.686(5)	Cu28–Se11	2.406(4)
Cu10–Se4	2.481(5)	Cu29–Se19	2.403(4)
Cu10–Se24	2.566(5)	Cu29–Se10	2.457(4)
Cu10–Se15	2.706(4)	Cu29–Se20	2.594(4)
Cu11–Se14	2.329(4)	Cu30–Se19	2.407(4)
Cu11–Se22	2.522(5)	Cu30–Se23	2.548(4)
Cu11–Se23	2.734(4)	Cu31–Se19	2.415(4)
Cu12–Se15	2.332(4)	Cu31–Se12	2.444(4)
Cu12–Se24	2.465(4)	Cu31–Se21	2.605(4)
Cu12–Se23	2.713(4)	Cu32–Se10	2.490(4)
Cu13–Se7	2.536(5)	Cu32–Se20	2.592(4)
Cu13–Se5	2.582(5)	Cu32–Se22	2.599(5)
Cu14–Se5	2.420(4)	Cu33–Se21	2.329(4)
Cu14–Se7	2.424(4)	Cu33–Se20	2.343(5)
Cu14–Se16	2.433(4)	Cu33–Se19	2.714(5)
Cu15–Se6	2.388(4)	Cu34–Se12	2.514(4)
Cu15–Se5	2.415(4)	Cu34–Se24	2.594(5)
Cu15–Se20	2.424(4)	Cu34–Se21	2.666(5)
Cu16–Se8	2.399(4)	Cu35–Se20	2.345(4)
Cu16–Se7	2.402(5)	Cu35–Se22	2.506(4)
Cu16–Se21	2.422(4)	Cu35–Se23	2.674(4)
Cu17–Se16	2.444(4)	Cu36–Se21	2.326(4)
Cu17–Se6	2.457(4)	Cu36–Se24	2.457(4)
Cu17–Se17	2.537(4)	Cu36–Se23	2.757(4)
Cu18–Se16	2.392(4)	S1–C84	1.79(3)
Cu18–Se23	2.534(4)	S2–C126	1.73(3)
Cu19–Se16	2.413(4)	Cu19–Se18	2.624(5)
Cu19–Se8	2.423(4)	Cu20–Se6	2.443(5)

dynamic light scattering experiments, and we attribute this to the bidentate ferrocenyldiselenolate ligands, as Cu–Se nanocluster complexes whose surfaces are passivated exclusively with phosphine ligands commonly display random condensation reactions when redissolved in organic solvents.<sup>7</sup> The good solubility and relative stability of cluster **3** in common organic solvents thus lends itself to an investigation of whether selective substitution reactions of the ancillary  $\text{PnPr}_3$  shell on such clusters could be performed, as the introduction of reactive groups via the phosphine ligand shell surrounding the cluster core may allow for covalent bonding of these clusters onto a metal surface.

Free thiol groups would be one of the most suitable candidates because their bonding behavior onto Au surfaces has been well studied.<sup>8</sup> Thiol phosphines, however, cannot be used directly in the preparation of Cu–Se clusters from

Cu(I) salts due to the reactive nature of the S–H bond.<sup>10,17</sup> For example, CuOAc reacts smoothly in solution with 2 equiv of the phosphinothiol  $\text{Ph}_2\text{P}(\text{CH}_2)_3\text{SH}$  to form  $\text{Cu}_2(\text{Ph}_2\text{P}(\text{CH}_2)_3\text{S})_2(\text{Ph}_2\text{P}(\text{CH}_2)_3\text{SH})_2$  (**4**) in 95% yield via activation of the S–H bond (and the elimination of HOAc). The dimeric complex **4** (Table 5) consists of two copper centers (Cu1 and the symmetry equivalent Cu1') each arranged in a pseudotetrahedral coordination geometry. Each copper is bonded to two thiolates (S1 and S1') and two phosphine ligands (Figure 4). One of the phosphine ligands (P1 and P1') acts as a bridging ligand, building a six-membered Cu–S–(CH<sub>2</sub>)<sub>3</sub>–P ring. The other phosphine ligands (P2, P2') complete the coordination about the metals, but retain a free thiol group. The copper–thiolate distances in **4** (2.3756(8)–2.3776(7) Å) are slightly longer than those reported for the related trinuclear complex  $[\text{CpFe}\{\eta^5\text{-C}_5\text{H}_5(1\text{-PPh}_2)(2\text{-CH}(\text{CH}_3)\text{S})\}\text{Cu}]_3$  (Cu–S = 2.178(6)–2.251(6) Å).<sup>17a</sup>

Using the preformed Cu–Se cluster **3**, however, we found that it is possible to incorporate thiol phosphine ligands as partial substitution of the  $\text{PnPr}_3$  ligand shell with  $\text{Ph}_2\text{P}(\text{CH}_2)_3\text{SH}$ , with the controlled, concomitant formation of a larger cluster framework. When cluster **3** was dissolved in mixture of diethyl ether and THF and treated with an excess of  $\text{Ph}_2\text{P}(\text{CH}_2)_3\text{SH}$ , a gradual lightening of the reaction solution was observed from which X-ray-quality dark brown needles of  $\text{Cu}_{36}(\text{Se}_2\text{fc})_6\text{Se}_{12}(\text{PnPr}_3)_{10}(\text{Ph}_2\text{P}(\text{CH}_2)_3\text{SH})_2$  (**5**) were isolated in 78% yield. The introduction of excess ligand resulted in a cluster expansion reaction, and there are clear structural relationships between the framework in **5** (Figure 5) and that displayed in **3**. The structure of  $\text{Cu}_{36}$  cluster **5** is best viewed as an expansion of the original  $\text{Cu}_{20}$  framework in **3**, albeit with a more condensed central core. Cluster **3** resides on a crystallographic inversion center and can be described as consisting of two  $\text{Cu}_{10}(\text{Se}_2\text{fc})_2\text{Se}_3$  units (Figure 6), and the larger framework in **5** can be viewed as being composed of three of these units (Figure 6) centered about a  $\text{Cu}_6\text{Se}_3$  core. The reduction in the  $\text{PR}_3:\text{Cu}$  ratio together with an increased ratio of  $\text{Se}^{2-}$  to surface  $\text{fcSe}_2^{2-}$  on going from **3** to **5** contributes to a more condensed core in **5**, with nine interstitial copper atoms coordinated by a  $\mu_9\text{-Se}$  ion (Se23) and two  $\mu_6\text{-Se}^{2-}$  centers (Se22 and Se24; Tables 6; Figure 5). As illustrated in Figure 5, two of the twelve phosphine ligands present are  $\text{Ph}_2\text{P}(\text{CH}_2)_3\text{SH}$  (bonded to Cu1 and Cu13), containing a free thiol group pointing out from the cluster surface. For the  $\text{Ph}_2\text{P}(\text{CH}_2)_3\text{SH}$  ligand P6, there is crystallographic evidence for a two-site  $\text{Ph}_2\text{P}(\text{CH}_2)_3\text{SH}:\text{PnPr}_3$  disorder, and a model with 70:30 occupancy of the two ligands gave a satisfactory refinement. The other tripropylphosphine ligands were ultimately not substituted.

(17) See for example: (a) Togni, A.; Rihs, G.; Blumer, R. E. *Organometallics* **1992**, *11*, 613–621. (b) Chen, C.-H.; Lee, G.-H.; Liaw, W.-F. *Inorg. Chem.* **2006**, *45*, 2307–2316. (c) Hsu, Hua-Fen; Peng, Wan-Yu; Li, Zung-Ying; Wu, Ru-Rong; Liao, Ju-Hsiou; Wang, Yu; Liu, Yi-Hung; Shieh, Minghuey; Kuo, Ting-Shen. *Inorg. Chim. Acta* **2005**, *358*, 2149–2154. (d) Matsuzaki, K.; Kawaguchi, H.; Voth, P.; Noda, K.; Itoh, S.; Takagi, H. D.; Kashiwabara, K.; Tatsumi, K. *Inorg. Chem.* **2003**, *42*, 5320–5329. (e) Ortner, K.; Hilditch, L.; Zheng, Y.; Dilworth, J. R.; Abram, U. *Inorg. Chem.* **2000**, *39*, 2801–2806. (f) Maina, T.; Pecorale, A.; Dolmella, A.; Bandoli, G.; Mazzi, U. *J. Chem. Soc., Dalton Trans.* **1994**, 2437–2443.

The direct assembly of the  $\text{Cu}_{36}\text{Se}_{12}(\text{fcSe}_2)_6$  framework observed in **5** can also be achieved using a combination of  $\text{CuOAc}\cdot\text{PnPr}_2\text{Ph}$ ,  $\text{Se}(\text{SiMe}_3)_2$ , and  $\text{fc}(\text{SeSiMe}_3)_2$ . The structurally related nanocluster  $\text{Cu}_{36}\text{Se}_{12}(\text{fcSe}_2)_6(\text{PnPr}_2\text{Ph})_{12}$  (**6**) can be prepared in crystalline form in good yield under low-temperature conditions (Supporting Information; Figure S1). This is perhaps not surprising, as the Tollman cone angles<sup>16</sup> for  $\text{PhPnPr}_2$  and  $\text{Ph}_2\text{P}(\text{CH}_2)_3\text{SH}$  are expected to be similar.

In summary, the ferrocenyldiselenide reagent  $\text{fc}(\text{SeSiMe}_3)_2$  is a convenient source for the delivery of  $\text{fcSe}_2^{2-}$  in the synthesis of Cu–Se cluster and nanocluster complexes. The bridging selenolate ligands impart a certain amount of kinetic stability to  $\text{Cu}_{20}\text{Se}_6(\text{fcSe}_2)_4(\text{PnPr}_3)_{10}$  (**3**). In the presence of excess  $\text{Ph}_2\text{P}(\text{CH}_2)_3\text{SH}$ , however, the cluster framework is selectively expanded to yield  $\text{Cu}_{36}(\text{Se}_2\text{fc}_2)_6\text{Se}_{12}(\text{PPR}_3)_{10}(\text{Ph}_2\text{P}(\text{CH}_2)_3\text{SH})_2$  (**5**), in which partial substitution of the  $\text{PPR}_3$  ligand shell has been achieved. This represents the first example of a structurally characterized nanocluster containing

phosphinothiol ligands and the first step en route to the assembly of copper–selenide nanoclusters that may be amenable to anchoring onto metal surfaces.

**Acknowledgment.** J.F.C. gratefully acknowledges the Natural Sciences and Engineering Research Council (NSERC) of Canada and the Government of Ontario Premier's Research Excellence Awards (PREA) program for financial support. J.F.C. also thanks the Forschungszentrum Karlsruhe for a visiting research fellowship. D.F. thanks the DFG Centre for Functional Nanostructures, the Fonds der Chemischen Industrie, and the Forschungszentrum Karlsruhe for financial support.

**Supporting Information Available:** X-ray crystallographic files in CIF format for complexes **1–6** including a representation of cluster **6** (Figure S1). This material is available free of charge via the Internet at <http://pubs.acs.org>.

IC061111N